

Effect of phenolic-hydroxy-group incorporation on the biological activity of a simplified aplysiatoxin analog with an (R)-(-)-carvone-based core

Ryo C. Yanagita^{a,*}, Yoshiyuki Suzuki^b, Yasuhiro Kawanami^a, Yusuke Hanaki^a, and Kazuhiro Irie^c

^aDepartment of Applied Biological Science, Faculty of Agriculture, Kagawa University, Kagawa 761-0795, Japan

^bDivision of Applied Biological and Rare Sugar Sciences, Graduate School of Agriculture, Kagawa University, Kagawa 761-0795, Japan

^cDivision of Food Science and Biotechnology, Graduate School of Agriculture, Kyoto University, Kyoto 606-8502, Japan

Corresponding Author

*(R.C.Y.) E-mail: yanagita.ryo@kagawa-u.ac.jp

ORCID 

Ryo C. Yanagita: 0000-0002-9217-5507



This is an Accepted Manuscript version of the following article, accepted for publication in *Bioscience, Biotechnology, and Biochemistry*.

Effect of phenolic-hydroxy-group incorporation on the biological activity of a simplified aplysiatoxin analog with an (R)-(-)-carvone-based core

Ryo C. Yanagita, Yoshiyuki Suzuki, Yasuhiro Kawanami, Yusuke Hanaki, and Kazuhiro Irie
Bioscience, Biotechnology, and Biochemistry, 2024, volume 88, issue 9, pages 992–998.
<https://doi.org/10.1093/bbb/zbae091>

It is deposited under the terms of the Creative Commons Attribution-NonCommercial-NoDerivatives License (<http://creativecommons.org/licenses/by-nc-nd/4.0/>), which permits non-commercial re-use, distribution, and reproduction in any medium, provided the original work is properly cited, and is not altered, transformed, or built upon in any way.

Keywords: Protein kinase C; Aplysiatoxin; Simplified analog; Antiproliferative activity; Relative binding free-energy calculation

ABSTRACT

We synthesized a phenolic hydroxy group-bearing version (**1**) of a simplified analog of aplysiatoxin comprising a carvone-based conformation-controlling unit. Thereafter, we evaluated its antiproliferative activity against human cancer cell lines and its binding affinity to protein kinase C (PKC) isozymes. The antiproliferative activity and PKC-binding ability increased with the introduction of the phenolic hydroxy group. The results of molecular dynamics simulations and subsequent relative binding free-energy calculations conducted using an alchemical transformation procedure showed that the phenolic hydroxy group in **1** could form a hydrogen bond with a phospholipid and the PKC. The former hydrogen bonding formation facilitated the partitioning of the compound from water to the phospholipid membrane and the latter compensated for the loss of hydrogen bond with the phospholipid upon binding to the PKC. This information may facilitate the development of rational design methods for PKC ligands with additional hydrogen bonding groups.

1 INTRODUCTION

Protein kinase C (PKC) isozymes belong to a family of serine/threonine kinases that represent potential targets for therapeutic drugs in the treatment of cancers, latent HIV eradication using the “shock and kill” strategy, and the treatment of Alzheimer’s disease.^{1,2} Natural tumor promoters, such as aplysiatoxin (ATX), bind to the tandem C1 domains (C1A and C1B) in both conventional (α , β I, β II, γ) and novel (δ , ϵ , η , θ) PKC isozymes and persistently activate them, leading to their downregulation. Given that loss-of-function mutations in PKC isozymes occur with many types of cancers, PKC isozymes are believed to continuously act as tumor suppressors.³ Consequently, therapeutic PKC activators should be carefully designed to avoid pan-PKC downregulation. Significant efforts have been dedicated to developing synthetic PKC ligands to address the limitations of the natural PKC activators.³ Our group reported simplified analogs of ATX (aplogs) (Figure 1), which exhibited antiproliferative activities without the tumor-promoting and proinflammatory activities characteristic of tumor promoters.^{4,5} A previous study has shown that molecular hydrophobicity is a key factor in the antiproliferative activity of aplogs,⁶ with a log P value of 4.0–4.5 being optimal for this activity. This is because high hydrophobicity facilitates the formation of a ternary complex involving the phospholipid membrane, ligand, and PKC C1 domain, whereas excessive hydrophobicity can hinder the ligand binding as the ligand becomes trapped within the hydrophobic region of the membrane. Additionally, the molecular hydrophobicity of the PKC ligands is associated with their tumor-promoting activity.⁷ Therefore, it is necessary that molecular hydrophobicity be carefully controlled when developing artificial PKC ligands.

In a previous study, we reported a synthetic analog of ATX featuring a conformation-controlling unit derived from (–)-carvone (aplog-CV1); it was synthesized in the longest linear sequence of 8 steps.⁸ However, this compound lacked a phenolic hydroxy group, which was predicted to form a hydrogen bond with the PKC C1 domains. This absence of the phenolic hydroxy group can enhance tumor-promoting activities. Conversely, introducing a hydrophilic group in an inappropriate position will increase desolvation energy upon binding and consequently reduce binding affinity. In this study, we synthesized aplog-CV2 (**1**), incorporating a phenolic hydroxy group in the same meta-position as natural ATXs, and evaluated its antiproliferative and PKC-binding activities.

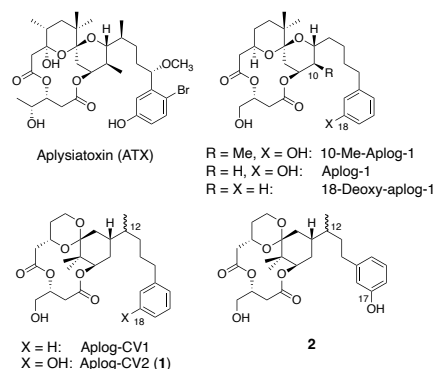


Figure 1: Structures of the aplysiatoxin and its simplified analogs.

2 RESULTS AND DISCUSSION

2.1 Synthesis of aplog-CV2 (1)

We synthesized **1** (Scheme S1) following the synthetic plan of aplog-CV1, wherein the side chain could be altered using a different olefin unit in the olefin cross-metathesis step. The longest linear sequence for the synthesis of **1** comprised 11 steps starting with the use of *m*-hydroxycinnamic acid, with an overall yield of 1.4%. Compound **2**, possessing a side-chain one-carbon short, was obtained through cross-metathesis involving 4-(*m*-benzyloxyphenyl)-2-butene, formed by catalytic olefin migration. Compounds **1** and **2** were separated by reversed-phase high-performance liquid chromatography (HPLC) and characterized as (3*S*)-isomers based on nuclear Overhauser effect spectroscopy (NOESY) experiments (Scheme S1). Similarly to aplog-CV1, the C-12 diastereomers could not be separated by HPLC. Consequently, biological evaluation was conducted using a diastereomeric mixture.

The *J*-values for the H-3 (doublet of doublets, 10.9, 2.6 Hz), H-8 (triplet, 3.6 Hz), and H-26 (doublet of doublets: 18.3, 4.0 Hz and 18.9, 11.5 Hz) of **1** were similar to those of aplog-CV1, suggesting that the phenolic hydroxy group did not affect the conformation of the macrocyclic ring.

Surprisingly, the retention times of aplog-CV1 (11.9 min) and **1** (12.0 min) in the reversed-phase HPLC (column, YMC-Pack ODS-AM AM12S05-1520WT; eluent, 87.5% MeOH/H₂O; flow rate, 8.0 mL min⁻¹) were similar. This result indicated that the phenolic hydroxy group did not decrease the molecular hydrophobicity. This outcome might be attributed to the potential formation of an intramolecular hydrogen bond between the phenolic hydroxy group and the carbonyl group at position **1**.

2.2 Antiproliferative activities toward human cancer cell lines

First, we evaluated the antiproliferative activities of **1** through an assay using a panel of 39 human cancer cell lines. The antiproliferative activity was quantified as the GI₅₀ value, representing the concentration required to inhibit cell growth by 50%, compared with the vehicle (control) group. Table 1 shows a list of the log GI₅₀ values of 18-deoxy-aplog-1,⁹ aplog-1,⁴ aplog-CV1,⁸ and **1** obtained for the PKC ligand-sensitive eight cancer cell lines (HBC-4, MDA-MB-231, SF-295, HCC2998, NCI-H460, A549, St-4, and MKN45). Comprehensive data for all 39 cancer cell lines are provided as Supplementary data (Table S1). Similar to other ATX analogs, **1** inhibited the growth of the eight cell lines at concentrations lower than 10⁻⁵ M. The Pearson's correlation coefficient, *r*, between the log GI₅₀ values of aplog-CV1 and **1** for the 39

cancer cell lines was as high as 0.73, suggesting that these compounds share the same target and mode of action: the activation of the PKC isozymes.

The mean $\log GI_{50}$ values of **1** and aplog-CV1 were -5.70 and -5.48 , respectively, indicating a higher antiproliferative activity of **1** for the cell lines than that of aplog-CV1. This result contradicted the observation that the antiproliferative activity of aplog-1 (mean $\log GI_{50}$ for the eight cell lines, -5.56) was slightly lower than that of 18-deoxy-aplog-1 (-5.76). Presumably, this inconsistency resulted from the similar molecular hydrophobicity of aplog-CV1 (t_R for octadecyl-silica (ODS) HPLC, 11.9 min) and **1** (t_R for ODS HPLC, 12.0 min); however, 18-deoxy-aplog-1 had higher molecular hydrophobicity (experimental $\log P_{ow}$, 4.8) than aplog-1 (experimental $\log P_{ow}$, 3.3).⁶

Table 1: Antiproliferative activities of 18-deoxy-aplog-1, aplog-1, aplog-CV1, and aplog-CV2 (**1**) toward eight human cancer cell lines

Cancer type		$\log GI_{50}$ (log M)			
		18-Deoxy-aplog-1 ^a	Aplog-1 ^b	Aplog-CV1 ^c	Aplog-CV2 (1)
Breast	HBC-4	-6.28	-6.33	-4.91	-6.21
	MDA-MB-231	-5.67	-5.61	-6.44	-5.52
Central nervous system	SF-295	-5.14	-5.06	-5.43	-5.31
Colon	HCC2998	-5.53	-5.43	-5.36	-5.53
Lung	NCI-H460	-5.83	-5.83	-5.82	-5.78
	A549	-5.49	-5.32	-5.49	-5.47
Stomach	St-4	-6.05	-5.55	-5.59	-5.44
	MKN45	-6.09	-5.33	-5.80	-6.33
Mean for the above 8 cell lines		-5.76	-5.56	-5.48	-5.70
MG-MID ^d of 39 cell lines		-5.09	-4.98	-5.02	-5.07

^a Data from Ref. 9. ^b Data from Ref. 4. ^c Data from Ref. 8. ^d The full panel mean graph midpoint (MG-MID) value, mean of the $\log GI_{50}$ values for all 39 human cancer cell lines.

2.3 Binding affinity toward PKC isozyme C1 domains

Next, we evaluated the binding affinity of **1** for PKC α and δ isozymes because the antiproliferative activity of aplogs toward cancer cell lines is associated with the activation of these isozymes.^{10,11} We employed the synthetic PKC α -C1A and δ -C1B peptides as surrogates for full-length PKC α and PKC δ , the primary binding domains of PKC ligands in each isozyme, in the [³H]phorbol 12,13-dibutyrate ([³H]PDBu) displacement assay.¹² In the assay, the binding affinity was expressed as a binding inhibition constant, K_i , which corresponded to a dissociation constant, K_d .

The binding ability of **1** for α -C1A (K_i , 11 nM) and δ -C1B (K_i , 6.1 nM) was approximately 8–10 times stronger than that of aplog-CV1 (K_i for α -C1A, 110 nM; for δ -C1B, 43 nM) (Table 2). When comparing aplog-1 with 18-deoxy-aplog-1, it was observed that the 18-OH group increased the binding affinity by only 2-fold (Table 2). Similarly, in other classes of PKC ligands, the removal of hydrogen bonds with carbonyl groups in the rim of the binding cleft did not diminish the binding affinity. For instance, the C4-deoxy analog of PDBu¹³ and the C9-deoxy analog of bryostatin-1¹⁴ exhibited binding affinities considerably similar to that of the corresponding parent compounds. These results can be attributed to the balance between hydrogen bonds and desolvation energies. Additionally, the formation of hydrogen bonds led to a decrease in conformational entropy upon binding.¹⁵ Therefore, it was unexpected to find that **1** exhibited a binding ability ten times higher than aplog-CV1.

Regarding the binding selectivity among PKC isozymes, **1** showed approximately 2-fold selectivity for δ -C1B over α -C1A, which was similar to that of aplog-CV1, indicating that the presence of phenolic hydroxy group had a negligible impact on the binding selectivity.

The binding ability of the one-carbon-short compound (**2**) was approximately 4 times lower than that of **1** but approximately 2 and 3 times higher than that of aplog-CV1 and 17-deoxy-**2** (K_i , 65 nM).⁸ The lower binding ability compared with **1** was consistent with the previous report showing that the ideal side-chain length is that of the natural product.¹⁶ The higher binding ability compared with aplog-CV1 and 17-deoxy-**2** suggested that, despite having a relatively short side chain linker, the phenolic hydroxy group of **2** could still form a hydrogen bond with the protein.

Table 2: Binding inhibition constants (K_i) for the inhibition of [³H]PDBu binding by 18-deoxy-Aplog-1, Aplog-1, Aplog-CV1, Aplog-CV2 (**1**), and **2**.

PKC C1 peptides	K_i (nM)				
	18-Deoxy-aplog-1 ^a	Aplog-1 ^b	Aplog-CV1 ^c	Aplog-CV2 (1)	2
α -C1A	120	63	110	11 (2) ^d	46 (2) ^d
δ -C1B	9.8	7.4	43	6.1 (0.6) ^d	22 (0) ^d

^a Data from Ref. 9. ^b Data from Ref. 4. ^c Data from Ref. 8. ^d Standard deviation from two separate experiments.

2.4 Molecular modeling study

To predict the role of the phenolic 18-OH group of **1** in binding to the PKC isozymes, we conducted the molecular dynamics (MD) simulations of the ligand-C1 domain complex within a 1-palmitoyl-2-oleoyl-*sn*-glycero-3-phospho-L-serine bilayer environment, employing a previously established method.¹⁶ For the simulation, a 12*S*-isomer of **1** (**CV2**) was chosen because of its identical configuration to natural ATXs. Initially, **CV2** was docked into the binding cleft of the PKC δ C1B domain. Subsequently, equilibration steps and a 5-ns of production run were performed at 300 K and 1 atm. In the predicted binding pose of **CV2** (Figure 2), the 18-OH group engaged in a hydrogen bond with a carbonyl group of Met-239, which resembled the interaction predicted in other phenol-bearing aplogs.

Next, we estimated the relative binding free-energy between a 12*S*-isomer of aplog-CV1 (**CV1**) and **CV2** using an “alchemical transformation” simulation:¹⁷ **CV1** was transformed into **CV2** via the two end states sharing a maximal common substructure (Figure S1). Specifically, the partial charge and van der Waals interaction of the H-18 atom of **CV1** gradually changed to zero, with the partial charge being incorporated into that of the C-18 atom to reach one end state. Similarly, the partial charges and van der Waals interactions of the 18-OH group of **CV2** gradually changed to zero, with the partial charges of all other atoms being gradually adjusted to those of the end state for **CV1** to reach the other end state. This alchemical transformation was conducted in three different settings: the ligand in water, at the membrane-water interface, and in complex with the PKC δ C1B domain and membrane. From these simulations, we estimated the relative free-energy changes of two different processes: water-to-membrane partition (process A) and binding of the protein-in-water to the membrane-embedded ligand (process B). The initial position and orientation of each ligand at the membrane-water interface were predicted using the Positioning of Proteins in Membranes (PPM) server. The free energy differences between the states were estimated using the multistate Bennett acceptance ratio method.

The relative free-energy change for process A ($\Delta\Delta G_{\text{partition}}$, ΔG for **CV1** – ΔG for **CV2**), water-to-membrane partition, was 1.01 kcal mol⁻¹ (Table S2), indicating that **CV2** preferred the membrane-water

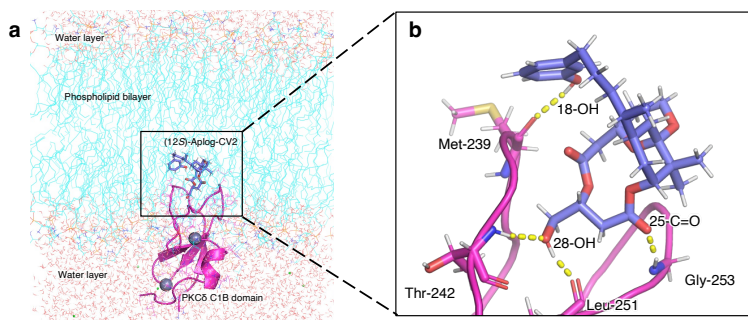


Figure 2: Predicted binding mode of **1** with the PKC δ -C1B domains: a) the side-view of the entire simulation box and b) a closeup of the ligand binding site. A 12S isomer of **1** (**CV2**) was used for the molecular dynamics simulation. Met-239, Thr-242, Leu-251, and Gly-253 are shown in the stick model. The intermolecular dashed lines represent hydrogen bonds. The backbone of the protein is shown in cartoon mode.

interface over the aqueous environment more than **CV1** did. During the simulation at the membrane–water interface, the phenolic 18-OH group of **CV2** stably formed a hydrogen bond with a *sn*-2 carbonyl group of the phospholipid. However, the primary 28-OH group formed relatively loose hydrogen bonds with a *sn*-3 oxygen atom of the phosphate linkage and water (Figure 3; for distance histogram, see Figure S2). This result suggests that the hydrogen bond between the 18-OH group and the phospholipid offers an advantage for the partition of **CV2** to the membrane–water interface.

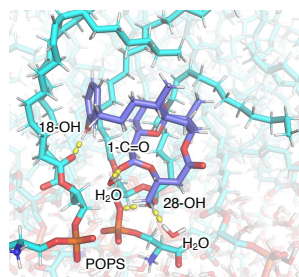


Figure 3: A snapshot from the molecular dynamics simulation of a 12S isomer of **1** (**CV2**) embedded in a 1-palmitoyl-2-oleoyl-*sn*-glycero-3-phospho-L-serine (POPS) bilayer membrane. The POPS and water molecules that interacted with **CV2** are highlighted. The intermolecular dashed lines represent hydrogen bonds.

The relative free-energy change for process B, $\Delta\Delta G_{\text{complex}}$, the ligand binding process within the membrane, was $-0.04 \text{ kcal mol}^{-1}$, indicating that the introduction of the 18-OH group slightly influenced the $\Delta\Delta G_{\text{complex}}$. Further, this result suggested that a hydrogen bond between the 18-OH of **CV2** and the Met-239 of the PKC δ C1B domain compensated for the loss of a hydrogen bond between the 18-OH group and the phospholipid. The overall relative binding free-energy between **CV1** and **CV2**, $\Delta\Delta G_{\text{bind}}$ ($\Delta\Delta G_{\text{partition}} + \Delta\Delta G_{\text{complex}}$), was $0.97 \text{ kcal mol}^{-1}$, which was approximately consistent with the experimental $\Delta\Delta G_{\text{bind}}$ for

δ -C1B, 1.16 kcal mol⁻¹ (calculated at 300 K).

We also estimated the relative binding free-energy between (12*S*)-17-deoxy-**2** and (12*S*)-**2** via the alchemical transformation procedure (Table S3). In contrast with **1**, $\Delta\Delta G_{\text{partition}}$ between (12*S*)-17-deoxy-**2** and (12*S*)-**2** was -0.568 kcal mol⁻¹, which indicated that (12*S*)-**2** preferred the aqueous environment over the membrane-water interface more than its 17-deoxy derivative did. $\Delta\Delta G_{\text{complex}}$ between (12*S*)-17-deoxy-**2** and (12*S*)-**2** was -0.168 kcal mol⁻¹, thus the overall relative binding free-energy was -0.736 kcal mol⁻¹. Although this value was qualitatively inconsistent with the experimental $\Delta\Delta G_{\text{bind}}$ for the PKC δ C1B peptide (0.65 kcal mol⁻¹) between 17-deoxy-**2** and **2**, this simulation implied that the shortening of side-chain linker length significantly changes the role of the phenolic hydroxy group in **2**, that is, it acts negatively in the membrane partition process and cannot form ideal hydrogen bond with the protein as **1**.

3 Conclusion

In this study, following a convergent synthetic route, we synthesized **1**, bearing a phenolic hydroxy group, in the longest linear sequence of 11 steps from commercially available *m*-hydroxycinnamic acid. Contrary to our expectations, **1** and aplog-CV1 had similar molecular hydrophobicity. However, **1** displayed higher antiproliferative activity toward human cancer cell lines and stronger binding ability to the PKC C1 domains than aplog-CV1. Particularly, **1** exhibited antiproliferative activities comparable to those of natural-product-resembling analogs, such as 18-deoxy-aplog-1 and aplog-1. These findings motivate the further optimization of the aromatic side chain of this facilely accessible carvone-based scaffold to yield potent and non-tumor-promoting PKC ligands in future studies.

Recent work by Pande's group revealed that different PKC ligands induce distinct positioning of the ligand-protein complex within the membrane in the MD simulations,¹⁸ suggesting that this variability may lead to diverse biological activities. Similarly, Lautala *et al.* reported that simulating PKC ligand-membrane interactions, including their positioning and orientation within the membrane, might aid in predicting their binding prospects.¹⁹ To date, the design and structure-activity relationship discussion of the PKC ligands have predominantly focused on interactions between ligands and proteins, often regarding the phenolic hydroxy group of ATXs simply as a hydrogen bonding moiety with the protein. Our deduction from the relative binding free-energy simulations suggested that the 18-OH group of **1**, initially hypothesized to solely serve as a hydrogen bond donor with the protein, significantly contributed to the partition of the ligand from water to membrane.

Regarding ligand-membrane interaction, Hirai *et al.* showed that the orientation of the hydrophobic side chain of ligands determines whether they activate the PKC isozyme or merely bind to the PKC isozyme without activation.²⁰ The simulation results of this study offer a novel perspective on the role of the hydrogen bonding groups of PKC ligands, specifically their potential roles in stabilizing the position of ligands at the membrane-water interface. This ligand positioning facilitates the formation of protein-ligand complexes. This hypothesis may aid in rationally tuning the position and orientation of the PKC ligands within the membrane.

4 Experimental

4.1 General remarks

The following spectroscopic and analytical instruments were used: ¹H and ¹³C NMR, JEOL JNM-ECZ500 (JEOL, Tokyo, Japan; internal standard, tetramethylsilane (0 ppm) for ¹H NMR and ¹³C NMR); HPLC, JASCO PU-4086 Semi-preparative pump with a JASCO UV-4075 UV/VIS Detector (JASCO, Tokyo, Japan); IR, FT/IR-670 Plus (JASCO, Tokyo, Japan); HR-ESI-TOF-MS, Xevo G2-XS (Waters, Tokyo, Japan) equipped with an ACQUITY UPLC BEH C18 column (Waters, Tokyo, Japan). High-performance

liquid chromatography was carried out on YMC-Pack ODS-AMAM12S05-1520WT (YMC, Kyoto, Japan). Wakogel C-300HG (silica gel, FUJIFILM Wako Pure Chemical Corporation, Osaka, Japan) were used for open and flash column chromatography. Preparative thin-layer chromatography was carried out on TLC Silica gel 60 F₂₅₄ (Merck KGaA, Darmstadt, Germany). [³H]PDBu (17.16 Ci/mmol) was custom-synthesized by PerkinElmer Life Science Research Products (Boston, MA, USA). The PKC C1 peptides were synthesized as reported previously.²¹ All other reagents were purchased from chemical companies and used without further purification. The experimental procedures for the synthesis of **1** and NMR data are provided as supplementary material.

4.2 Measurements of cell growth inhibition

A panel of 39 human cancer cell lines established by Yamori *et al.*²² was employed. The cells were seeded on 96-well plates in Roswell Park Memorial Institute 1640 (RPMI-1640) medium supplemented with 5% fetal bovine serum and allowed to attach overnight. After the cell was incubated with **1** for 48 h, cell growth was estimated by sulforhodamine B assay. The 50% growth inhibition (GI₅₀) parameter was calculated as reported previously.²² Absorbance for the control well (*C*) and the test well (*T*) was measured at 525 nm along with that for the test well at time 0 (*T*₀). Cell growth inhibition (% growth) by each concentration of **4** (10⁻⁸, 10⁻⁷, 10⁻⁶, 10⁻⁵ and 10⁻⁴) was calculated as 100[(*T* - *T*₀)/(*C* - *T*₀)] using the average of duplicate points. By processing of these values, GI₅₀ value, defined as 100[(*T* - *T*₀)/(*C* - *T*₀)] = 50, was determined.

4.3 Inhibition of specific binding of [³H]PDBu to PKC C1 peptides

The binding of [³H]PDBu to the PKCα-C1A and δ-C1B peptides was evaluated by the procedure of Sharkey and Blumberg,¹² with modification as reported previously,²³ using 50 mM Tris-maleate buffer (pH 7.4 at 4 °C), 40 nM PKCα-C1A or 13.8 nM PKCδ-C1B peptides, 20 nM [³H]PDBu (17.16 Ci/mmol), 50 μg/mL 1,2-dioleoyl-*sn*-glycero-3-phospho-L-serine, 3 mg/mL bovine γ-globulin, and various concentrations of **1** and **2**. Binding affinity was determined based on the concentration required to cause 50% inhibition of specific binding of [³H]PDBu (IC₅₀), which was calculated by logit procedure. The inhibition constant (*K*_i) was calculated by the Goldstein-Barrett equation, $K_i = IC_{50}/(2 \times [L_{50}]/[L_0] - 1 + [L_{50}]/K_d)$, where [*L*₅₀] is a free [³H]PDBu concentration at 50% inhibition, [*L*₀] is a free [³H]PDBu concentration in the absence of non-labelled ligand, and *K*_d is a dissociation constant of [³H]PDBu. The smaller values (13.11 Ci mmol⁻¹) of the specific activity of [³H]PDBu were used for the calculation in consideration of radioactive decay.

4.4 MD simulations

Docking simulation and setup for the molecular dynamics (MD) simulation were performed as described previously,¹⁶ using Avogadro,²⁴ OpenBabel,²⁵ AutoDock-GPU (version 4.2.6),²⁶ MGLTools (1.5.7 RC1), the Swiss PDB Viewer,²⁷ the CHARMM-GUI Bilayer Builder,^{28,29} the PPM server (version 3.0),³⁰ and the AmberTools22 package.³¹ The AMBER ff14SB force field, the Zinc AMBER Force Field (ZAFF), the LIPID21 force field, and the GAFF2 force field were used to describe the system. The restrained electrostatic potential (RESP) charges for ligands were computed using Gaussian16 (Revision C.02) program at the B3LYP/6-31+(d,p)//HF/6-31(d) level of theory, alongside the AmberTools22 package. For membrane-containing systems, a rectangular simulation box was filled by TIP3P water. *Z*-length of the simulation box was determined by water thickness (minimum water height on top and bottom of the system was set to 22.5 Å), and initial *XY*-lengths were set to 62 Å. The net charge on the system was neutralized by adding 150 mM of KCl. For the ligand in water system, a rhombic dodecahedron box (with a solute-to-box distance of 12 Å) was used, and the 150 mM of KCl was added. All MD simulations were performed

Acknowledgements

The DFT and RHF calculations were performed using Research Center for Computational Science, Okazaki, Japan (Project: 23-IMS-C255).

References

- [1] Youry Kim, Jenny L. Anderson, and Sharon R. Lewin. Getting the “Kill” into “Shock and Kill”: Strategies to Eliminate Latent HIV. *Cell Host and Microbe*, 23(1):14–26, 2018.
- [2] Alexandra C. Newton. Protein kinase C: perfectly balanced. *Critical Reviews in Biochemistry and Molecular Biology*, 53(2):208–230, mar 2018.
- [3] Yu Nakagawa. Artificial analogs of naturally occurring tumor promoters as biochemical tools and therapeutic leads. *Bioscience, Biotechnology, and Biochemistry*, 76(7):1262–1274, 2012.
- [4] Yu Nakagawa, Ryo C. Yanagita, Naoko Hamada, Akira Murakami, Hideyuki Takahashi, Naoaki Saito, Hiroshi Nagai, and Kazuhiro Irie. A simple analogue of tumor-promoting aplysiatoxin is an antineoplastic agent rather than a tumor promoter: Development of a synthetically accessible protein kinase C activator with bryostatin-like activity. *Journal of the American Chemical Society*, 131(22):7573–7579, 2009.
- [5] Kazuhiro Irie, Masayuki Kikumori, Hiroaki Kamachi, Keisuke Tanaka, Akira Murakami, Ryo C. Yanagita, Harukuni Tokuda, Nobutaka Suzuki, Hiroshi Nagai, Kiyotake Suenaga, and Yu Nakagawa. Synthesis and structure-activity studies of simplified analogues of aplysiatoxin with antiproliferative activity like bryostatin-1. *Pure and Applied Chemistry*, 84(6):1341–1351, 2012.
- [6] Hiroaki Kamachi, Keisuke Tanaka, Ryo C. Yanagita, Akira Murakami, Kazuma Murakami, Harukuni Tokuda, Nobutaka Suzuki, Yu Nakagawa, and Kazuhiro Irie. Structure-activity studies on the side chain of a simplified analog of aplysiatoxin (aplog-1) with anti-proliferative activity. *Bioorganic and Medicinal Chemistry*, 21(10):2695–2702, 2013.
- [7] Yusuke Hanaki, Masayuki Kikumori, Harukuni Tokuda, Mutsumi Okamura, Shingo Dan, Naoko Adachi, Naoaki Saito, Ryo C. Yanagita, and Kazuhiro Irie. Loss of the Phenolic Hydroxyl Group and Aromaticity from the Side Chain of Anti-Proliferative 10-Methyl-aplog-1, a Simplified Analog of Aplysiatoxin, Enhances Its Tumor-Promoting and Proinflammatory Activities. *Molecules*, 22(4):631, apr 2017.
- [8] Yoshiyuki Suzuki, Keiichi Moritoki, Mizuki Kajiwara, Ryo C. Yanagita, Yasuhiro Kawanami, Yusuke Hanaki, and Kazuhiro Irie. Design, synthesis, and biological activity of a synthetically accessible analog of aplysiatoxin with an (*R*)-(-)-carvone-based conformation-controlling unit. *Bioscience, Biotechnology, and Biochemistry*, 86(8):1013–1023, 2022.
- [9] Ryo C. Yanagita, Hiroaki Kamachi, Keisuke Tanaka, Akira Murakami, Yu Nakagawa, Harukuni Tokuda, Hiroshi Nagai, and Kazuhiro Irie. Role of the phenolic hydroxyl group in the biological activities of simplified analogue of aplysiatoxin with antiproliferative activity. *Bioorganic and Medicinal Chemistry Letters*, 20(20):6064–6066, 2010.
- [10] Yusuke Hanaki, Yuki Shikata, Masayuki Kikumori, Natsuki Hotta, Masaya Imoto, and Kazuhiro Irie. Identification of protein kinase C isozymes involved in the anti-proliferative and pro-apoptotic activities of 10-Methyl-aplog-1, a simplified analog of debromoaplysiatoxin, in several cancer cell lines. *Biochemical and Biophysical Research Communications*, 495(1):438–445, 2018.
- [11] Marcelo G. Kazanietz and Mariana Cooke. Protein kinase C signaling “in” and “to” the nucleus: Master kinases in transcriptional regulation. *Journal of Biological Chemistry*, 300(3):105692, 2024.

- [12] Nancy A. Sharkey and Peter M. Blumberg. Highly lipophilic phorbol esters as inhibitors of specific [³H]phorbol 12,13-dibutyrate binding. *Cancer Research*, 45:19–24, 1985.
- [13] Minoru Tanaka, Kazuhiro Irie, Yu Nakagawa, Yoshimasa Nakamura, Hajime Ohigashi, and Paul A. Wender. The C4 hydroxyl group of phorbol esters is not necessary for protein kinase C binding. *Bioorganic & Medicinal Chemistry Letters*, 11(5):719–722, mar 2001.
- [14] Gary E. Keck, Yam B. Poudel, Arnab Rudra, Jeffrey C. Stephens, Noemi Kedei, Nancy E. Lewin, Megan L. Peach, and Peter M. Blumberg. Molecular modeling, total synthesis, and biological evaluations of C9-deoxy bryostatin 1. *Angewandte Chemie - International Edition*, 49(27):4580–4584, 2010.
- [15] Maria Luisa Verteramo, Olof Stenström, Majda Misini Ignjatović, Octav Caldararu, Martin A. Olsson, Francesco Manzoni, Hakon Leffler, Esko Oksanen, Derek T. Logan, Ulf J. Nilsson, Ulf Ryde, and Mikael Akke. Interplay between Conformational Entropy and Solvation Entropy in Protein–Ligand Binding. *Journal of the American Chemical Society*, 141(5):2012–2026, feb 2019.
- [16] Atsuko Gonda, Koji Takada, Ryo C. Yanagita, Shingo Dan, and Kazuhiro Irie. Effects of side chain length of 10-methyl-aplog-1, a simplified analog of debromoaplysiatoxin, on PKC binding, anti-proliferative, and pro-inflammatory activities. *Bioscience, Biotechnology, and Biochemistry*, 85(1):168–180, 2021.
- [17] Solmaz Azimi, Sheenam Khuttan, Joe Z. Wu, Rajat K. Pal, and Emilio Gallicchio. Relative Binding Free Energy Calculations for Ligands with Diverse Scaffolds with the Alchemical Transfer Method. *Journal of Chemical Information and Modeling*, 62(2):309–323, jan 2022.
- [18] Steven M. Ryckbosch, Paul A. Wender, and Vijay S. Pande. Molecular dynamics simulations reveal ligand-controlled positioning of a peripheral protein complex in membranes. *Nature Communications*, 8(1):6, feb 2017.
- [19] Saara Lautala, Riccardo Provenzani, Ilari Tarvainen, Katia Sirna, S. Tuuli Karhu, Evgeni Grazhdankin, Antti K. Lehtinen, Hanan Sa’d, Artturi Koivuniemi, Henri Xhaard, Raimo K. Tuominen, Virpi Talman, Alex Bunker, and Jari Yli-Kauhaluoma. Expanding the Paradigm of Structure-Based Drug Design: Molecular Dynamics Simulations Support the Development of New Pyridine-Based Protein Kinase C-Targeted Agonists. *Journal of Medicinal Chemistry*, 66(7):4588–4602, apr 2023.
- [20] Go Hirai, Adashi Shimizu, Toru Watanabe, Yosuke Ogoshi, Megumi Ohkubo, and Mikiko Sodeoka. Importance of interaction between C1 domain and lipids in protein kinase C α activation: Hydrophobic side chain direction in isobenzofuranone ligands controls enzyme activation level. *ChemMedChem*, 2(7):1006–1009, 2007.
- [21] Kazuhiro Irie, Kentaro Oie, Akifumi Nakahara, Yoshiaki Yanai, Hajime Ohigashi, Paul A. Wender, Hiroyuki Fukuda, Hiroaki Konishi, and Ushio Kikkawa. Molecular basis for protein kinase C isozyme-selective binding: The synthesis, folding, and phorbol ester binding of the cysteine-rich domains of all protein kinase C isozymes. *Journal of the American Chemical Society*, 120(36):9159–9167, 1998.
- [22] Takao Yamori, Akio Matsunaga, Shigeo Sato, Kanami Yamazaki, Akiko Komi, Kazuhiro Ishizu, Izumi Mita, Hajime Edatsugi, Yasuhiro Matsuba, Kimiko Takezawa, Osamu Nakanishi, Hiroshi Kohno, Yuki Nakajima, Hironori Komatsu, Toshio Andoh, and Takashi Tsuruo. Potent antitumor activity of MS-247, a novel DNA minor groove binder, evaluated by an *in vitro* and *in vivo* human cancer cell line panel. *Cancer Research*, 59(16):4042–4049, 1999.
- [23] Ryo C. Yanagita, Mao Otani, Satoshi Hatanaka, Hiroto Nishi, Shota Miyake, Yusuke Hanaki, Masashi Sato, Yasuhiro Kawanami, and Kazuhiro Irie. Analysis of binding mode of vibsantin A with protein kinase C C1 domains: An experimental and molecular dynamics simulation study. *Journal of Molecular Structure*, 1260:132866, 2022.

- [24] Marcus D. Hanwell, Donald E. Curtis, David C. Lonie, Tim Vandermeersch, Eva Zurek, and Geoffrey R. Hutchison. Avogadro: an advanced semantic chemical editor, visualization, and analysis platform. *Journal of Cheminformatics*, 4:17, 2012.
- [25] Noel M O’Boyle, Michael Banck, Craig A James, Chris Morley, Tim Vandermeersch, and Geoffrey R Hutchison. Open Babel: An open chemical toolbox. *Journal of Cheminformatics*, 3(1):33, dec 2011.
- [26] Garrett M. Morris, Ruth Huey, William Lindstrom, Michel F. Sanner, Richard K. Belew, David S. Goodsell, and Arthur J. Olson. AutoDock4 and AutoDockTools4: Automated Docking with Selective Receptor Flexibility. *Journal of Computational Chemistry*, 30(16):2785–2791, 2009.
- [27] Nicolas Guex and Manuel C. Peitsch. SWISS-MODEL and the Swiss-PdbViewer: an environment for comparative protein modeling. *Electrophoresis*, 18(15):2714–23, dec 1997.
- [28] Sunhwan Jo, Taehoon Kim, Vidyashankara G. Iyer, and Wonpil Im. CHARMM-GUI: A Web-based Graphical User Interface for CHARMM. *Journal of Computational Chemistry*, 29:1859–1865, 2008.
- [29] Jumin Lee, Xi Cheng, Jason M. Swails, Min Sun Yeom, Peter K. Eastman, Justin A. Lemkul, Shuai Wei, Joshua Buckner, Jong Cheol Jeong, Yifei Qi, Sunhwan Jo, Vijay S. Pande, David A. Case, Charles L. Brooks, Alexander D. MacKerell, Jeffery B. Klauda, and Wonpil Im. CHARMM-GUI Input Generator for NAMD, GROMACS, AMBER, OpenMM, and CHARMM/OpenMM Simulations using the CHARMM36 Additive Force Field. *Journal of Chemical Theory and Computation*, 12(1):405–413, 2016.
- [30] Mikhail A. Lomize, Irina D. Pogozheva, Hyeon Joo, Henry I. Mosberg, and Andrei L. Lomize. OPM database and PPM web server: Resources for positioning of proteins in membranes. *Nucleic Acids Research*, 40(D1):D370–D376, 2012.
- [31] D.A. Case, H.M. Aktulga, K. Belfon, I.Y. Ben-Shalom, J.T. Berryman, S.R. Brozell, D.S. Cerutti, T.E. Cheatham, III, G.A. Cisneros, V.W.D. Cruzeiro, T.A. Darden, R.E. Duke, G. Giambasu, M.K. Gilson, H. Gohlke, A.W. Goetz, R. Harris, S. Izadi, S.A. Izmailov, K. Kasavajhala, M.C. Kaymak, E. King, A. Kovalenko, T. Kurtzman, T.S. Lee, S. LeGrand, P. Li, C. Lin, J. Liu, T. Luchko, R. Luo, M. Machado, V. Man, M. Manathunga, K.M. Merz, Y. Miao, O. Mikhailovskii, G. Monard, H. Nguyen, K.A. O’Hearn, A. Onufriev, F. Pan, S. Pantano, R. Qi, A. Rahnamoun, D.R. Roe, A. Roitberg, C. Sagui, S. Schott-Verdugo, A. Shajan, J. Shen, C.L. Simmerling, N.R. Skrynnikov, J. Smith, J. Swails, R.C. Walker, J. Wang, J. Wang, H. Wei, R.M. Wolf, X. Wu, Y. Xiong, Y. Xue, D.M. York, S. Zhao, and P.A. Kollman. AMBER2022, 2022.
- [32] Mark James Abraham, Teemu Murtola, Roland Schulz, Szilárd Páll, Jeremy C. Smith, Berk Hess, and Erik Lindah. Gromacs: High performance molecular simulations through multi-level parallelism from laptops to supercomputers. *SoftwareX*, 1-2:19–25, 2015.
- [33] Michael R. Shirts and Andrew L. Ferguson. Statistically Optimal Continuous Free Energy Surfaces from Biased Simulations and Multistate Reweighting. *Journal of Chemical Theory and Computation*, 16(7):4107–4125, jul 2020.